Experiments in Atmospheric Predictability: Part II. Data Assimilation

WILLIAM BLUMEN

Department of Astro-Geophysics, University of Colorado, Boulder 80309

(Manuscript submitted 27 May 1975)

The divergent barotropic model presented in Part I is used to investigate reduction of rms forecast errors by periodic updating with model-produced observations. Results show that an asymptotic error level is reached in about 2 days. This rapid adaptation reflects the initial balancing provided to the data at each update. Asymptotic rms forecast errors are increasing functions of both the updating period and the observation error, but the asymptotic error level is shown to be independent of the initial error. These results are in basic agreement with experiments carried out with various numerical models. Error reduction by statistically optimal assimilation of data is expected to yield results similar to those obtained in a previous study by the author.

1. Introduction

The predictability experiments, described in Part I of this study (Blumen 1976), provide quantitative information on the growth rate of errors and range of atmospheric predictability when initialization procedures are, to some degree, incompatible with true atmospheric properties, with the forecast model, or both. The results, based on a divergent barotropic model, are shown to be in basic agreement with results obtained with complex numerical models of the atmosphere. The doubling time for typical errors is typically less than one week, a period which effectively serves as the predictability range for numerical models in current use. It is hoped that increased four-dimensional space and time observational coverage will provide a viable means of improving the accuracy and extending the range of prediction. Optimal techniques of using these data have been actively pursued, following experiments by Charney *et al.* (1969). These experiments demonstrated that periodic insertion of correct or (small) error-contaminated temperature data into a numerical atmospheric model provides a means to recover the wind field, which was incorrectly specified at the initial time. The rms error of the wind field decreased with time, reaching an asymptotic value by about 3 weeks. The asymptotic error level reached was shown to increase with the error introduced into the temperature data, meant to simulate errors in meteorological observations. The experiment performed by Charney and colleagues has been repeated and extended with other numerical models, with basic agreement in the results obtained. Bengtsson (1975) has provided a survey of the simulation experiments performed to date and critically evaluated the results.

The techniques that have been used in most four-dimensional assimilation (updating) experiments generally fall into three classes: (i) direct insertion of correct temperatures *or* winds, but not both, (ii) direct insertion as in (i) but with random errors added to the data assimilated, and (iii) statistical data assimilation. The approach under (i) and (ii) is essentially that provided by Charney and colleagues, often with variants added: these include balancing procedures, to attain an initial adjustment between the mass and momentum fields, the use of real data with its inherent errors, and updating by sectors to simulate assimilation of satellite data. The statistical approach is generally one in which the model prediction and the data used for insertion (the observations) are provided relative weights at each assimilation period, according to the error inherent in each data source, in order to provide the optimal estimate of the true field. This latter procedure, referred to as weighted assimilation, has also been reviewed by Bengtsson.

In the present study, results from a number of updating experiments will be presented, which illustrate procedures in each of the three classes listed above. The purpose of these experiments is to analyze features of four-dimensional data assimilation that do not depend on the use of a particular numerical algorithm to solve the model system of equations. The control state and forecast solutions are analytically determined from the model equations developed in Part I of this study. In Sections 2 and 3 updating procedures, with and without random "observation" errors, will be analyzed in terms of initialization error, updating frequency, and scale of the planetary wave disturbance. Application of statistical assimilation is discussed in Section 4. Mathematical details, leading to results displayed in Sections 2 and 3, appear in the Appendices.

2. Updating with observations

The model, control state and forecast solution employed in Part I will be utilized throughout the

present analysis. In particular, the control streamfield is given by

$$\Psi_c(x,y,\tau)=\cos(kx+\sigma\tau+ly)+\cos(kx+\sigma\tau-ly), \quad (1)$$

where the (k,l) denote (x,y) wavenumbers and σ, the planetary wave frequency, is given by (8) in Part I. As in Part I, the amplitude ψ_f of the initial streamfield, used to balance the initial pressure field π, is assumed to be in error. The amplitudes of this streamfield are $\hat{a}_1(0)=\hat{a}_2(0)=1+\epsilon$, where the initial error ϵ is a random variable with a rectangular probability distribution. In order to reduce the rms prediction error, arising from this initial error, periodic updating of the streamfield will be carried out. The "observations" used for updating are defined as

$$\Psi^0=(1+\epsilon_n^0)\Psi_c, \quad (2)$$

where ϵ_n^0 denotes a random observation with zero mean value and n is an index referring to an update. The observational errors are assumed to be statistically independent [see (11)]. From this point, the analysis proceeds as in Sections 3 and 4 of Part I. The approximate solution satisfying the initial condition, determined from the balance equation [Part I, Eq. (15)] and (2), is

$$\begin{aligned}\Psi(x,y,\tau)=&[a_2(0)\sin\gamma\tau+a_1(0)\cos\gamma\tau]\\&\times\cos(kx+\sigma\tau+ly)+[-a_1(0)\sin\gamma\tau\\&+a_2(0)\cos\gamma\tau]\cos(kx+\sigma\tau-ly)\\&-\mathrm{Ro}\hat{a}_1(0)\hat{a}_2(0)bk^2\cos 2ly, \quad (3)\end{aligned}$$

where

$$\gamma=\mathrm{Ro}\hat{a}_1(0)\hat{a}_2(0)ab\lambda^2lk^3(k^2-3l^2), \quad (4)$$

$\mathrm{Ro}\lesssim 0.1$ denotes the Rossby number, and $\hat{a}_1(0)$ and $\hat{a}_2(0)$ denote amplitudes of the initial streamfield

$$\left.\begin{aligned}a_1(0)&=\{(1+\epsilon_0^0)-a[(1+\epsilon_0^0)-\hat{a}_1(0)]\}\\a_2(0)&=\{(1+\epsilon_0^0)-a[(1+\epsilon_0^0)-\hat{a}_2(0)]\}\end{aligned}\right\}, \quad (5)$$

$$a=[1+\lambda^2(k^2+l^2)]^{-1}, \quad (6)$$

$$b=[1+4\lambda^2l^2]^{-1}. \quad (7)$$

The dimensionless radius of deformation λ, defined in terms of reduced gravity g', bottom layer depth D_0, characteristic quarter-wavelength L, and constant Coriolis parameter f_0, is given by

$$\lambda=(g'D_0)^{\frac{1}{2}}f_0^{-1}L^{-1}. \quad (8)$$

Time τ and λ are normalized with parameter values characteristic of midlatitude flow such that $\lambda^2(k^2+l^2)=1$ and one day corresponds to $\tau=1$.

At time $\tau=\Delta\tau$, the predicted streamfield is $\Psi(x,y,\Delta\tau)$, given by (3); the observed field at this time is $\Psi^0=(1+\epsilon_1^0)\Psi_c(x,y,\Delta\tau)$, where Ψ_c is given by (1). The initialization procedure that led to the forecast solution (3) is again repeated. In general, this updating procedure may be carried out $(N+1)$ times until an asymptotic value of the rms forecast error is essentially reached. This error, given by (26) in Part I, is

$$\begin{aligned}r(N\Delta\tau)=\tfrac{1}{2}\{&[1-a_1(N\Delta\tau)]^2+[1-a_2(N\Delta\tau)]^2\\&+[a_3(N\Delta\tau)]^2\}^{\frac{1}{2}}, \quad (9)\end{aligned}$$

where the expressions for the $a_i(N\Delta\tau)$ are displayed in Appendix A.

First we shall consider the case when the observations are perfect ($\epsilon_n^0\equiv 0$), so that $\Psi^0\equiv\Psi_c$. The expected value of the rms forecast error becomes

$$\begin{aligned}&(\langle[r(N\Delta\tau)]^2\rangle)^{\frac{1}{2}}\\&\approx\{\langle[(X_{N-1}+aX_{N-2}+a^2X_{N-3}+\cdots+a^{N-1}X_0)\\&\quad+\epsilon a^N(X_{N-1}+X_{N-2}+X_{N-3}+\cdots+X_0)]^2\rangle\\&\qquad+\langle(\epsilon a^N)^2\rangle+\tfrac{1}{2}\langle[a_3(N\Delta\tau)]^2\rangle\}^{\frac{1}{2}}, \quad (10)\end{aligned}$$

where a is defined by (6), while X_N and $a_3(N\Delta\tau)$ are given by (A4) and (A3) in Appendix A. Since the initial error ϵ is represented by a rectangular probability distribution, the statistical average, denoted by the angle brackets, may easily be determined at time $\tau=N\Delta\tau$. Some results, for various error bounds α, are shown in Fig. 1.

The results shown in Fig. 1 are in agreement with earlier results, based on a linear analysis, presented by Blumen (1975a): the asymptotic error level is essentially independent of the initial errors but is an increasing function of the update period $\Delta\tau$. Although gravity-inertia waves have been removed after each update, simulating damping of high-frequency motions, the present results are similar to experimental results obtained with numerical models. It would appear that interaction between gravity-inertia and planetary waves is not significant, at least during the relatively short period between updates. Experiments carried out with the NCAR GCM have been reported by Williamson and Kasahara (1971); a survey of up-to-date results has been provided by Bengtsson (1975).

The length of time to reach the asymptotic error level in the present experiment is typically 1–2 days. Typical times in the NCAR GCM experiments range from about one to two weeks with or without observational errors included. However, Kistler and McPherson (1975) performed updating experiments in which a local balancing procedure was adopted. Forecast winds at each grid point were replaced by a corrected wind, composed of the predicted ageostrophic component and an analyzed geostrophic component, determined from a known height field. It is clear, from their results, that this balancing procedure accelerates the adjustment toward an asymptotic error level in comparison to the corresponding rate of adjustment without local balancing of the wind field. In principle, a similar approach has been employed here. At each update the pressure field is constrained to satisfy the balance equation. As a consequence, the initial wind field is composed of

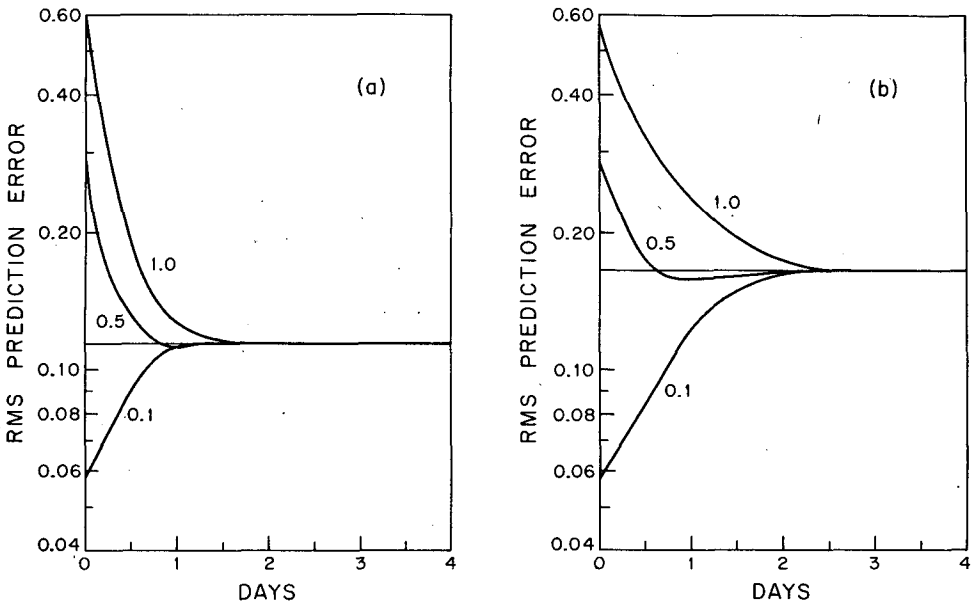

FIG. 1. Model rms prediction error, defined by (10), from updating every 6 h (a) and every 12 h (b) with perfect observations. The three curves correspond to the maximum amplitude error bounds $|\alpha| = 0.1$, 0.5 and 1.0. Parameter values are: $a=0.5$, $b=0.333$, $\gamma=0.1$, Ro$=0.1$. The initial rms error is $(\alpha/3)^{\frac{1}{2}}$.

both a balanced and an unbalanced component. Thus, it seems clear that the discrepancy between the results shown in Fig. 1 and those reported by Williamson and Kasahara are primarily related to the initialization procedure adopted. Williamson and Kasahara inserted observations directly, without initial balancing, allowing the model to achieve its own state of balance.

The asymptotic error level is reached when the rate of adjustment of the mass and wind fields, determined by the model dynamics, is equal to the model-determined growth rate of initial errors. An initialization procedure that is capable of accelerating this adjustment process will, as a consequence, provide a more rapid means to counteract the growth of initial errors. It is apparent that the balancing procedure employed by Kistler and McPherson, and the approach used in the present model, provided a mass/wind relationship that was sufficiently close to the true state of the model that the adjustment of the residual imbalance proceeded rapidly. In particular, the initial imbalance in the present model is order Ro$\ll$1 from the true initial state.

The present results, together with results from numerical experiments that employ some form of initialization (see Bengtsson, 1975), suggest that an initialization procedure that accelerates the dynamical mass-wind adjustment will prove to be a more fruitful area for numerical experimentation than simple insertion of observational data.

3. Asymptotic error

Most numerical experiments indicate that the time to reach adaptation to an error level is essentially independent of observational errors assimilated into the model. This result is also produced by the present model; some typical results have previously been displayed by Blumen (1975b). Further, it has been established, also in agreement with numerical model experimentation, that the asymptotic error level is essentially independent of the error in the initial state. Consequently, only the asymptotic error level will be considered, when the present model is updated with error contaminated observations, given by (2).

We again make use of the angle bracket notation to denote a statistical average. The probability distribution of the observational errors is not specified, but their statistical independence is incorporated into the analysis:

$$\left.\begin{aligned}\langle \epsilon_n^0 \epsilon_m^0 \rangle &= 0, \quad n \neq m \\ \langle (\epsilon_n^0)^2 \rangle &= \langle (\epsilon^0)^2 \rangle \neq 0\end{aligned}\right\}. \tag{11}$$

An accurate value of the asymptotic rms forecast error, for $\Delta\tau \lesssim 12$ h, is developed in Appendix B and is given by

$$\begin{aligned}\lim_{N\to\infty} (\langle [r(N\Delta\tau)]^2 \rangle)^{\frac{1}{2}} &\equiv E^{(\infty)} \\ &\approx \left\{ (\gamma\Delta\tau)^2 \left[\frac{1}{(1-a)^2(1-b)^2} + 2\left(\frac{1-a}{1+a}\right) \langle (\epsilon^0)^2 \rangle \right.\right. \\ &\quad \left.\times \left(\frac{1}{(1-a)(1-b)} + \frac{2(1+ab)}{(1-a^2)(1-b^2)(1-ab)} \right) \right] \\ &\quad + \frac{1-a}{1+a} \langle (\epsilon^0)^2 \rangle + \tfrac{1}{2} (\mathrm{Ro}\, bk^2)^2 \left[\frac{1}{(1-b)^2} + 2\left(\frac{1-a}{1+a}\right) \langle (\epsilon^0)^2 \rangle \right. \\ &\quad \left.\left.\times \left(\frac{1}{1-b} + \frac{2(1+ab)}{(1-b^2)(1-ab)} \right) \right] \right\}^{\frac{1}{2}},\end{aligned} \tag{12}$$

where $\langle(\epsilon^0)^2\rangle$ is given by (11) and γ; and a and b are defined in (4), (6) and (7): $a, b, \neq 1$.

The contribution to the rms error from the presence of a nonlinear exchange process is reflected by the terms proportional to $(\gamma\Delta\tau)^2$, for the propagating waves, and to Ro^2, for the zonal flow. In each case, the existence of an observational error increases the forecast error. The remaining term, which only depends on the parameter $a=[1+\lambda^2(k^2+l^2)]^{-1}$ and the observation error, reflects the linear response to updating the forecast model [cf. Blumen, 1975b; Eq. (10)]. Numerical evaluation of (12) shows that for updating intervals equal to or less than 12 h ($\Delta\tau \lesssim 0.5$) and for observations that are not in error by more than 50% ($\langle(\epsilon^0)^2\rangle^{\frac{1}{2}} \lesssim 0.5$), the rms forecast error for midlatitude synoptic-scale flow is approximately

$$E^{(\infty)} \approx \left\{\left[\frac{\gamma\Delta\tau}{(1-a)(1-b)}\right]^2 + \frac{1-a}{1+a}\langle(\epsilon^0)^2\rangle + \frac{1}{2}\left[\frac{\mathrm{Ro}\, bk^2}{1-b}\right]^2\right\}^{\frac{1}{2}}. \quad (13)$$

When $\langle(\epsilon^0)^2\rangle^{\frac{1}{2}} > 0.2$, the contribution from the observational error is larger than from each of the other two terms; when $\langle(\epsilon^0)^2\rangle^{\frac{1}{2}} > 0.5$,

$$E^{(\infty)} \approx \left\{\frac{1-a}{1+a}\langle(\epsilon^0)^2\rangle\right\}^{\frac{1}{2}}. \quad (14)$$

The evaluation of $E^{(\infty)}$, given by (12) as a function of the rms observation error $p \equiv \langle(\epsilon^0)^2\rangle^{\frac{1}{2}}$ is displayed in Fig. 2. Fig. 3 shows $E^{(\infty)}$ as a function of the updating interval when $p=0$. The asymptotic rms zonal wind error from temperature and surface reference pressure updating with the NCAR GCM was estimated from the results obtained by Williamson and Kasahara (1971, Fig. 4). The dashed line connects normalized values obtained for 6 and 12 h updating periods. Although there is rough correspondence between the monotonic increase of $E^{(\infty)}$ with $\Delta\tau$, insufficient values of $E^{(\infty)}$ were available from the NCAR GCM experiments to verify a linear relationship.

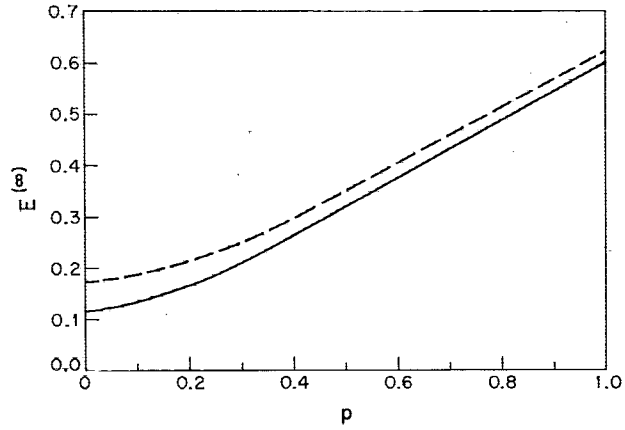

FIG. 2. Asymptotic rms prediction error $E^{(\infty)}$ as a function of the rms observation error p for 6 (solid) and 12 h (dashed) updating periods. The parameter values are given in Fig. 1.

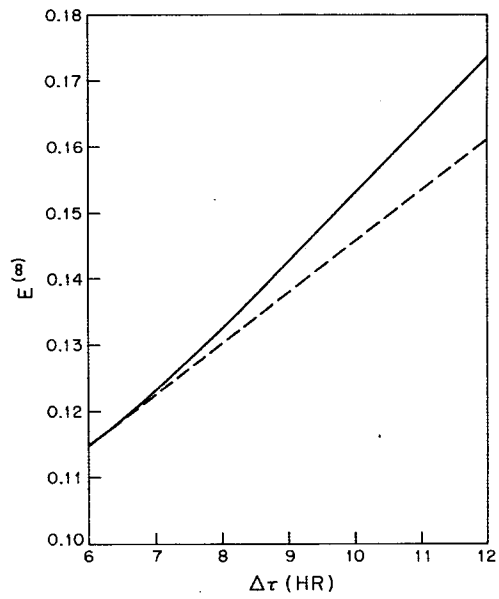

FIG. 3. Asymptotic rms prediction error $E^{(\infty)}$ as a function of the updating period $\Delta\tau$ (solid). The dashed line represents a result from the NCAR GCM experiments discussed in the text.

In summary, the present results show that the asymptotic error level increases with the observation error and with the period between updates. The relationship is given by (12) or (13). Actual observation errors are of order 0.1, so that nonlinear energy exchange and differences in propagation speed between model and atmospheric disturbances (Blumen, 1975b) are responsible for most of the contribution to the rms forecast error. For cases when the observation errors are small, Fig. 3 shows that more frequent updating would essentially reduce the error variance in direct proportion to $\gamma\Delta\tau$, the product of the nonlinear growth rate of the present model and the updating interval. To the extent that the above conclusions could be extended to meteorological conditions for which $\mathrm{Ro} \gg 0.1$ has not been determined. However, it is noteworthy that the present results are in basic agreement with rms forecast errors determined from *global models*. In particular, either the rms forecast errors in tropical regions show a similar dependence on updating interval and observation errors, the global rms error is heavily weighted by midlatitude error characteristics, or a combination of both features occurs.

4. Remarks

Statistical techniques for data assimilation have, to date, been based on multiple linear regression schemes. Blumen (1975b) has examined rms forecast errors, using such a scheme, with a linear representation of the divergent barotropic model used in the

present study. In this latter study, the statistically optimal assimilation of initial data produced an optimal forecast, in view of the linearity of the model dynamics. Although the present model permits nonlinear energy exchange, the wave amplitudes are governed by a system of linear equations (see Part I, Appendix). As a consequence, application of linear statistical assimilation to the present case would produce forecast error reduction similar to the results found earlier by Blumen. More generally, the forecast provided by a nonlinear triad solution will not be optimal unless optimal estimates of the quadratic terms are specified. A dynamical method to predict second-moment statistics is required to overcome the latter problem. This, in turn, implies the need for a satisfactory closure scheme. Bengtsson (1975) has noted, in this regard, that present approaches to this problem are usually too time-consuming for operational use.

The properties of the present model solutions have provided reasonably good agreement with predictability and updating experiments carried out with more complex numerical models. As emphasized in Sections 2 and 3, the dependence of error growth and its control on initialization, updating interval, and observational errors can be isolated and displayed in a relatively simple manner. Consequently, the greater insight to model response, that can be gained from a relatively simple analytical approach, suggests further application of this approach to the problems of forecast error reduction.

Acknowledgments. Discussions with Akira Kasahara have been both stimulating and helpful in clarifying many points raised in both parts of this paper. This investigation was supported by the Atmospheric Science Section of the National Science Foundation, under Grant GA-31868.

APPENDIX A

Wave Amplitudes

The wave amplitudes in (9) are determined by periodic updating of the forecast solution with observed data. At time $\tau=N\Delta\tau$, the amplitudes are:

$$\begin{aligned}a_1(N\Delta\tau)\approx{}&(1-a)\{(1+\epsilon^0_{N-1})(1+X_{N-1})\\&+a(1+\epsilon^0_{N-2})(1+X_{N-1}+X_{N-2})\\&+a^2(1+\epsilon^0_{N-3})(1+X_{N-1}+X_{N-2}+X_{N-3})\\&+\cdots+a^{N-1}(1+\epsilon^0_0)(1+X_{N-1}+\cdots+X_0)\}\\&+a^N\hat{a}_2(0)(X_{N-1}+X_{N-2}+\cdots+X_0)+a^N\hat{a}_1(0)\end{aligned}\tag{A1}$$

$$\begin{aligned}a_2(N\Delta\tau)\approx{}&(1-a)\{(1+\epsilon^0_{N-1})(1-X_{N-1})\\&+a(1+\epsilon^0_{N-2})(1-X_{N-1}-X_{N-2})\\&+a^2(1+\epsilon^0_{N-2})(1-X_{N-1}-X_{N-2}-X_{N-3})\\&+\cdots+a^{N-1}(1+\epsilon^0_0)(1-X_{N-1}-\cdots-X_0)\}\\&-a^N\hat{a}_1(0)(X_{N-1}+X_{N-2}+\cdots+X_0)+a^N\hat{a}_2(0)\end{aligned}\tag{A2}$$

$$\begin{aligned}a_3(N\Delta\tau)={}&\mathrm{R}o bk^2\{a_1[(N-1)\Delta\tau]a_2[(N-1)\Delta\tau]\\&+ba_1[(N-2)\Delta\tau]a_2[(N-2)\Delta\tau]\\&+b^2a_1[(N-3)\Delta\tau]a_2[(N-3)\Delta\tau]\\&+\cdots+b^{N-1}\hat{a}_1(0)\hat{a}_2(0)\}.\end{aligned}\tag{A3}$$

Here a and b are given by (6) and (7), the observational errors ϵ^0_n are defined by (2), and $\hat{a}_1(0)$ and $\hat{a}_2(0)$ are initial amplitude errors. The notation X_n denotes

$$X_n=\gamma(n\Delta\tau)\Delta\tau,\tag{A4}$$

where $\Delta\tau$ is the updating interval, and

$$\begin{aligned}\gamma[(N-1)\Delta\tau]={}&\mathrm{R}o\gamma(0)\\&\times\{a_1[(N-1)\Delta\tau]a_2[(N-1)\Delta\tau]\\&+ba_1[(N-2)\Delta\tau]a_2[(N-2)\Delta\tau]\\&+b^2a_1[(N-3)\Delta\tau]a_2[(N-3)\Delta\tau]\\&+\cdots+b^{N-1}\hat{a}_1(0)\hat{a}_2(0)\},\end{aligned}\tag{A5}$$

with $\gamma(0)$ being defined by (4) with $\hat{a}_1(0)=\hat{a}_2(0)\equiv 1$.

In the development of $a_1(N\Delta\tau)$ and $a_2(N\Delta\tau)$, the following simplification has been introduced:

$$\cos(X_{N-1})=1-\frac{(X_{N-1})^2}{2!}+\cdots\approx 1,$$

$$\sin(X_{N-1})=X_{N-1}-\frac{(X_{N-1})^3}{3!}+\cdots\approx X_{N-1},$$

where $X_{N-1}<0.1$ if $\Delta\tau\leqslant 0.5$.

APPENDIX B

Asymptotic Root Mean Square Forecast Error

The derivation of (12) is developed from the expression for $r(N\Delta\tau)$, given by (9), where the wave amplitudes are displayed in Appendix A. The statistical average of $[r(N\Delta\tau)]^2$ is carried out by making use of the assumed statistical independence of the observation errors, expressed by (11). The derivation is exceedingly long and details will not be presented. The full expression for the limiting value ($N\to\infty$) of the rms forecast error consists of geometric series whose sums are easily established. Simplifications are based on: $(X_n)^2\ll 1$, where X_n is given by (A4), $\langle(\epsilon^0_n)^4\rangle$ is neglected in comparison with $\langle(\epsilon^0_n)^2\rangle$, and $a<1$, $b<1$. Numerical evaluation of the result (12) shows that the reduced form, given by (13), is sufficiently accurate for present purposes. The accuracy of the latter is confirmed by computing $\langle\langle[r(N\Delta\tau)]^2\rangle\rangle^{\frac{1}{2}}$, for $\epsilon^0_n\equiv 0$, as a function of N until the asymptote is essentially reached. The asymptotic expression presented in (13) agrees with the numerical result to within 2% when $\Delta\tau=0.25$ and to within 5% when $\Delta\tau=0.50$. This small error can be traced to the approximation introduced at the end of Appendix A.

REFERENCES

Bengtsson, L., 1975: Four-dimensional assimilation of meteorological observations. GARP Publ. Ser., No. 15, WMO-ICSU Joint Organizing Committee, 76 pp.

Blumen, W., 1975a: An analytical view of updating meteorological variables: Part I. Phase errors. *J. Atmos. Sci.*, **31**, 274–286.

——, 1975b: An analytical view of updating meteorological variables: Part II. Weighted assimilation. *J. Atmos. Sci.*, **32**, 690–697.

——, 1976: Experiments in atmospheric predictability: Part I. Initialization. *J. Atmos. Sci.*, **33**, 161–169.

Charney, J., M. Halem and R. Jastrow, 1969: Use of incomplete historical data to infer the present state of the atmosphere. *J. Atmos. Sci.*, **26**, 1160–1163.

Kistler, R. E., and R. D. McPherson, 1975: On the use of a local wind correction technique in four-dimensional data assimilation. *Mon. Wea. Rev.*, **103**, 445–449.

Williamson, D., and A. Kasahara, 1971: Adaptation of meteorological variables forced by updating. *J. Atmos. Sci.*, **20**, 1313–1324.